THE CONSTRUCTION OF THE COMBUSTION MODELS FOR RME BIO-DIESEL FUEL FOR ICE APPLICATION

Valeri I. Golovitchev and Junfeng Yang

(Department of Applied Mechanics, Chalmers University of Technology, S-412 96, Göteborg, Sweden)

ABSTRACT

Bio-diesel fuels refer to non-petroleum based diesel fuels consisting of long chain alkyl esters produced by transesterifcation of vegetable oils, and proposed to be used (as neat or blended with conventional fuels) in unmodified diesel engines. Currently, there are few papers (see e.g. [1,2]) in which theoretical models for bio-diesel (e.g. RME) combustion simulations were reported. The models, developed in this paper, are modifications of those described in [1]. After the compilation of liquid fuel properties, the existing detailed mechanism of methyl butanoate ester, $C_5H_{10}O_2$ [2, 3] oxidation was supplemented by sub-mechanisms for two proposed fuel constituent components, C_7H_{16} and C_7H_8O (and, then, by mp2d and propyne, C_3H_4) to represent the combustion model of RME described by the chemical formula, $C_{19}H_{34}O_2$ (or $C_{19}H_{36}O_2$). The main fuel vapor thermal properties were taken as those of methyl palmitate $C_{19}H_{36}O_2$ in the NASA polynomial form of the Burcat [4] database. The special global reaction was introduced to "crack" the main fuel into constituent components, which sub-mechanisms were collected in the general (309 species, 1472 reactions) including also soot and NO_x formation processes. The detailed combustion mechanism was validated using shock-tube ignition-delay data at diesel engine conditions. For constant volume and diesel engine (Volvo D12C) combustion modeling, this mechanism was reduced to 88 species participating in 363 reactions.

Keywords: bio-diesel, comprehensive chemical kinetic mechanisms, ignition delay times, emissions formations.

INTRODUCTION

Bio-diesel fuels refer to non-petroleum based diesel fuels consisting of long chain alkyl esters produced by transesterifcation of vegetable oils, and proposed to be used (as neat or blended with conventional fuels) in unmodified diesel engines. Bio-diesel is the name given to the esters which are supposed to be used in diesel engine. The esters have the structure R-(C=O)-O-R', where R and R' are chains of alkyl and alkenyl groups with as many as 17-19 carbon atoms. The five components of the typical bio-diesel fuel are: methyl palmitate ($C_{17}H_{34}O_2$), methyl stearate ($C_{19}H_{38}O_2$), methyl oleate ($C_{19}H_{36}O_2$), methyl linoleate ($C_{19}H_{34}O_2$) and methyl linolenate ($C_{17}H_{32}O_2$); the average content of them are shown in Tab.1.

Esters	Formulas	Soybean biodiesel	Rapeseed biodiesel, RME
methyl palmitate	$C_{17}H_{34}O_2$	6-10%	4.3%
methyl stearate	$C_{19}H_{38}O_2$	2-5%	1.3%
methyl oleate	$C_{19}H_{36}O_2$	20-30%	59,9%
methyl linoleate	$C_{19}H_{34}O_2$	50-60%	21.1%
methyl linolenate	$C_{19}H_{32}O_2$	5-11%	13.2%

Table.1: Average compositions of soybean and rapeseed bio-diesels, see [5]

Due to the extra oxygen atoms contained in the molecules, carbons atoms are expected to have higher oxidized rate. It means lower carbon monoxide, CO, emissions can be achieved. Since bio-diesel molecules are long chain large molecules, to describe the oxidation process a large chemical mechanism is needed. Currently, there are few papers (see e.g. [1-3, 5]) in which theoretical mechanisms for bio-diesel combustion were developed.

In this paper, the combustion of Rapeseed Methyl Ester, RME, has been studied. The chemical model, developed is a modification of the approach described in [1]. The existing detailed mechanism of methyl butanoate ester [2] oxidation was supplemented by sub-mechanisms for supposed fuel constituent components, C_7H_{16} and C_7H_8O to represent combustion of RME, $C_{19}H_{34}O_2$ or $C_{19}H_{36}O_2$ when md, mb and C_3H_4 were selected. The main liquid fuel properties were taken as those of methyl oleate, $C_{19}H_{36}O_2$ [6]. These property data were successfully compared with the similar information presented in [7] which has been calculated using different real gas models described in [8]. The main fuel vapor thermal properties were taken as those of methyl palmitate $C_{19}H_{36}O_2$ in the NASA polynomial form of the Burcat [4] database. The global reaction was introduced to "crack" the main fuel into constituent components, which sub-mechanisms were collected in the general (309 species, 1472 reactions) one which includes also soot and NO_x formation processes. Bio-diesel auto-ignition properties were validated using constant volume and shock tube data at diesel engine conditions. For spray combustion applications, the detailed mechanism has been reduced to 88 species participating in 363 reactions. This mechanism has been used to investigate combustion and emissions (NO_x and soot) formation/oxidation in the research diesel engine (Volvo D12C). The comparison was made with engine performance and the emission formations for conventional diesel oil. The 3-D engine simulations have been carried out using KIVA-3V engine combustion code modified for detailed chemistry applications.

MODEL FORMULATION

Bio-diesel fuel physical properties

To model the spray atomization, droplets breakup and evaporation, and finally, combustion of RME, its physical properties are compiled. The properties of methyl oleate ($C_{19}H_{36}O_2$) have been "adapted" to represent those of RME. The fuel parameters are listed in Tab.2:

molecular weight (kg/kmol)	critical temperature (K)	critical pressure (Pa)	critical volume (m³/kmol)	normal boiling point (K)	IG heat of formation (J/kmol)
296.494	764.0	1.28E+06	1.06	617.0	-6.26E+08

Table.2: Main property parameters of methyl oleate ($C_{19}H_{36}O_2$)

This information can be used to estimate the physical properties required for numerical simulations: fuel enthalpy, latent heat of vaporization, vapor pressure, liquid viscosity, surface tension and thermal conductivity. A part of information can be found in the Dortmund Data Bank, DDB, [9], which can be used for research and application problems. For our purposes, the Data Compilation [6] has been employed to calculate the required bio-diesel physical properties.

The other methods employed, e.g. in [7, 10] to derive the physical properties of bio-diesel have been listed in Tab.3. A part of these models was used for a selected comparison with the values calculated using the approximations presented in [6].

Properties	Methods	Properties	Methods
Surface Tension	Estimated by Sugden's method [11]	Vapor Pressure	Data predicted by Riedel's method used in regression [11]
Liquid Viscosity	Data predicted by VanVelzen's method used in regression [11]	Liquid Thermal Conductivity	Data predicted by Baroncini's method used in regression [12]
Latent Heat of Vaporization	Data predicted by Clapeyron's method used in regression [11]	Enthalpy	Data predicted by [13]

Table.3: The methods used to estimate the physical properties of RME in [6]

The physical properties of primary reference component of diesel oil (hexadecane, $C_{16}H_{34}$), diesel oil surrogate ($C_{14}H_{28}$) [14] and RME have been compared in Fig.1.
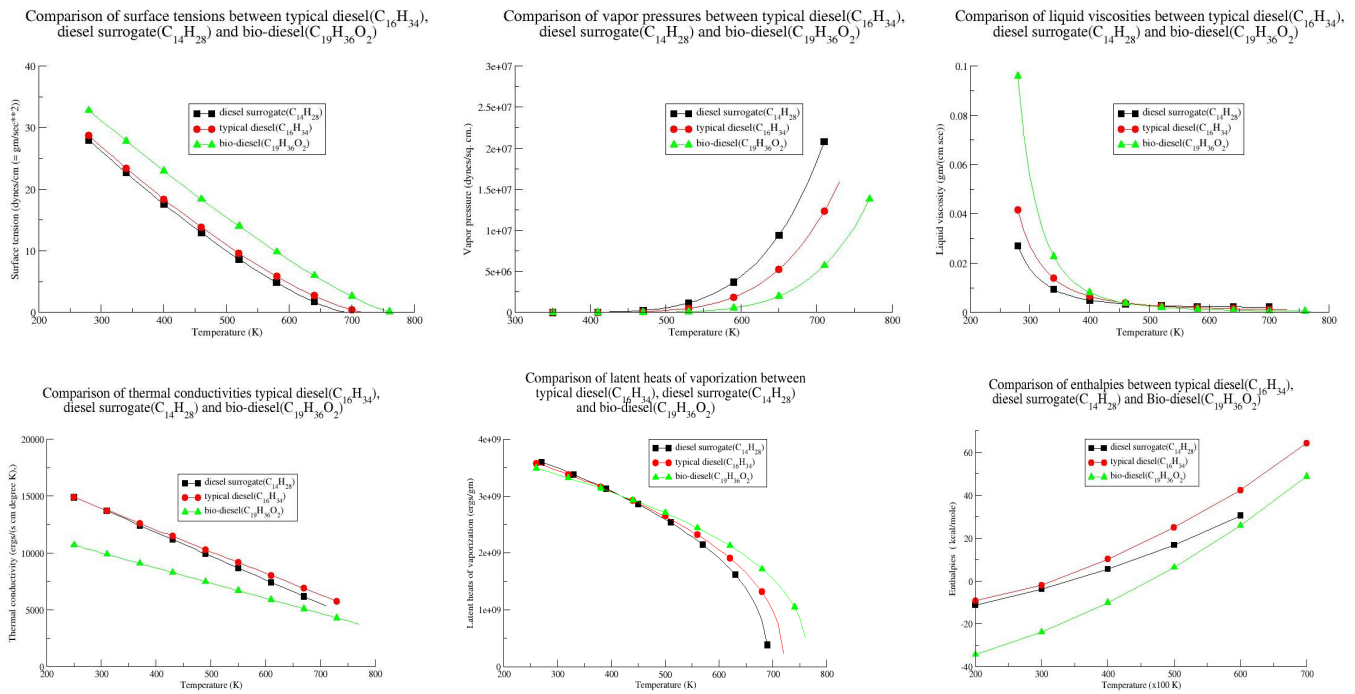

Figure.1: Comparison of physical properties of different diesel fuels

All these data tabulated as functions of temperature are included in the fuel library of the KIVA-3V code [15] used in the simulations. The difference among the properties is not drastic that opens the prospect to use RME in the diesel engines without hardware modifications. To compare the properties calculated using different methods, only the latent heat of vaporization and vapor pressure have been selected and presented in Fig.2. From this comparison follows the methods for fuel properties calculation must be carefully selected.

Turbulent Combustion Modeling

KIVA-3V code solves time-dependent conservation laws of a turbulent, chemical reactive flow of ideal gases, coupled to the equations for single-component vaporizing fuel sprays. To simulate turbulent combustion, the Partially Stirred Reactor (PaSR) method [16] has been employed. To outline the main
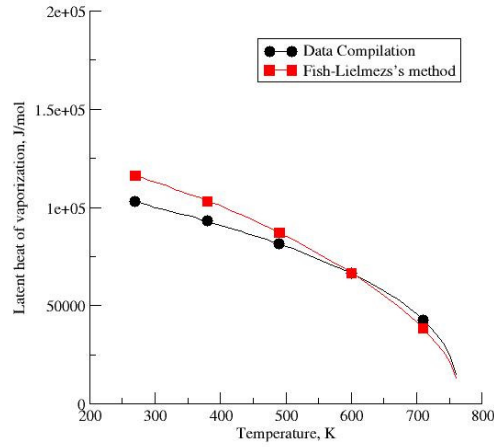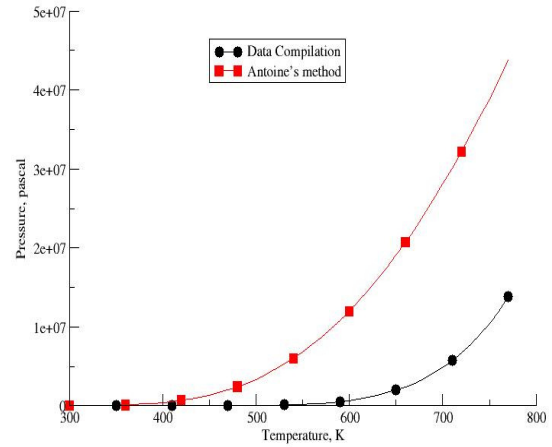
Figure.2 The comparison between RME property data calculated using different methods

features of the approach let us consider the average gas phase equations for a chemically reacting mixture of ideal gases with embedded condensed liquid droplets can be written as

$$\frac{\partial \rho_i}{\partial t} + \nabla \left[\rho_i \bar{u} - \frac{\mu_t}{Sc_i} \nabla \rho_i \right] = \dot{\rho}_i^c + \delta_{i1} \dot{\rho}_i^s, \qquad i = 1,..., N_s \tag{1}$$

where ρ_i is the density of the i-species, $\dot{\rho}_i^c$ is the chemical sources term defined by combustion mechanism, $\delta_{i1} \dot{\rho}_i^s$ is the source term due to the presence of spray, δ_{i1} is the Kronecker delta function, i.e. species 1 is the species of which the spray droplets are composed; μ_t is the turbulent viscosity and Sc_i is the Schmidt number, N_s is the number of species.

Since the KIVA-3V code is based on the operation-splitting procedure applied to the mass conservation equations Eq. (1) for species participating in any multi-step reaction mechanism, the third step of the computational procedure accounts for chemical kinetics coupled with micro-mixing. This step can be interpreted as representing combustion in a constant volume partially stirred reactor of a computational cell size, where reactions occur in a fraction of its volume described in the term of the system of ODEs.

$$\frac{dc^1}{dt} = f_r(...,c,...), \tag{2}$$

where $f_r(...,c,...)$ is the chemical source term calculated using, at some unknown (virtual) species molar densities, c, the parameters of a sub-grid scale reaction zone. The species indices are omitted for simplicity.

To close the model, the additional equation for the reaction volume can be used

$$\frac{dc}{dt} = -\frac{c - c^1}{\tau_{mix}} + f_r(...,c,...), \tag{3}$$

where τ_{mix} is the micro-mixing time.
The model distinguishes between the concentration at the reactor exit, c^1, the concentration in the reaction zone, c, and in the feed, c^0. When time proceeds, c^1 trades place for c^0.

The difference between Eq. (3) and the equation from the PSR (Perfectly Stirred Reactor) [17] model is that the residence time in the reactor equation of the PSR model is replaced by the micro-mixing time. Taking Eq. (3) in a steady-state form, one can get the basic equations of the PaSR model as follows

$$\frac{dc}{dt} = f_r(c) = \frac{c - c^1}{\tau_{mix}} \tag{4}$$

There are a number of micro-mixing models based on different principles; the review of these can be found in [18]. One of the simplest and widely used micro-mixing model is the "Interaction by Exchange with the Mean"(IEM) approach [19]. In this approach, the scalar variable c relaxes to its mean c^1 value according to the linear term in the equation Eq. (4).Then, rewriting the reaction rate $f_r(c)$ in Eq. (4) in terms of reactor exit parameters, one can get

$$f_r(c^1) + (\partial f_r / \partial c)_{|c=c^1} (c - c^1) = f_r(c^1) - \frac{c - c^1}{\tau_c} \tag{5}$$

using the Taylor's expansion at the value c^1, assuming that the reaction times can be estimated as a reciprocal value of the Jacobian matrix elements evaluated at the grid resolved values $c=c^1$, i.e., $\tau_c \sim [\partial f_r / \partial c]^{-1}$ and accounting for that $(\partial f_r / \partial c)_{|c=c^1} < 0$. Algebraic manipulation with the second pair of Eq. (5) leads to the relation

$$f_r(c^1) - \frac{c - c^1}{\tau_c} = \frac{c - c^1}{\tau_{mix}} \tag{6}$$

and finally to the main rate expression of the PaSR model.

$$f_r(c) = f_r(c^1) \frac{\tau_c}{\tau_c + \tau_{mix}} \tag{7}$$

This means the chemical source terms can be calculated using the averaged species concentrations, if multiplied by the model rate parameter ratio $\tau_c / (\tau_c + \tau_{mix})$. The application of Eq. (7) to the chemical mechanism of an arbitrary complexity is straightforward.

Bio-diesel Surrogate Combustion Mechanisms

The long chain methyl ester, $C_{19}H_{34}O_2$ will generate a lot of species during the combustion process. The reaction mechanism was proposed in a form of a bio-diesel surrogate, a blend which is assumed to be a 1:1:1 (volume ratio) mixture of n-heptane (C_7H_{16}), Methl Butanoate (mb, $C_5H_{10}O_2$) and Phenyl Methyl Ether (pme, C_7H_8O). Mb represents the short chain ester; pme − the cylic compounds; n-heptane − a long chain alkyl groups. To describe the bio-diesel surrogate decomposition into constituent components, one global stage was introduced:

$$C_{19}H_{34}O_2 + 0.5O_2 \Rightarrow C_7H_{16} + C_5H_{10}O_2 + C_7H_8O$$
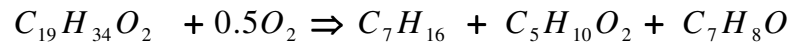
The detailed sub-mechanisms for three constituent components are existing. The mb mechanism [3] taken from the LLNL web site contains 264 species participating in 1219 reactions. The n-heptane and pme sub-mechanisms were taken in the form [20] involving 72 species and 325 reactions. Combined together, this leads to the RME mechanism consisting of 309 species taking in part 1472 reactions. For engine combustion applications, the mechanism was reduced to 88 species taking in part 363 reactions. Such mechanism is comparable in size with that described in [1]. All sub-mechanisms matched the shock-tube and flame propagation experimental data for constituent components.

Chemical Mechanism Validation

The chemical sub-mechanisms for RME constituent components, n-heptane, pme (toluene data were used), were validated using shock-tube and flame propagation experimental data and the comparison results were reported in [21]. The mb sub-mechanism was validated against the experimental data on the flame propagation at atmospheric pressure and different initial temperatures published in [22], as shown in Fig. 3. The predicted pressure dependence of the flame propagation velocity is presented in Fig. 4.
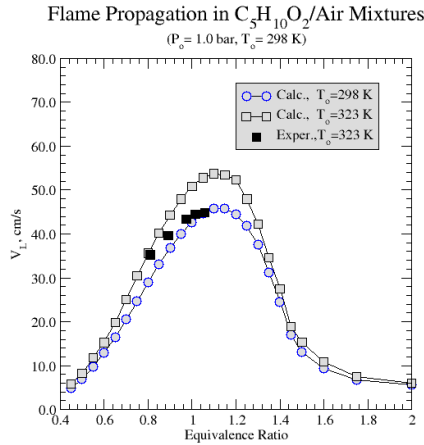
Figure.3: Comparison of predicted and measured flame propagation velocities for mb/air stoichiometric mixture
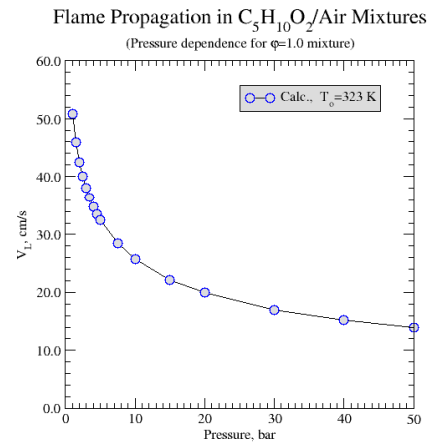
Figure.4: The pressure dependence of the predicted mb/air flame propagation velocity

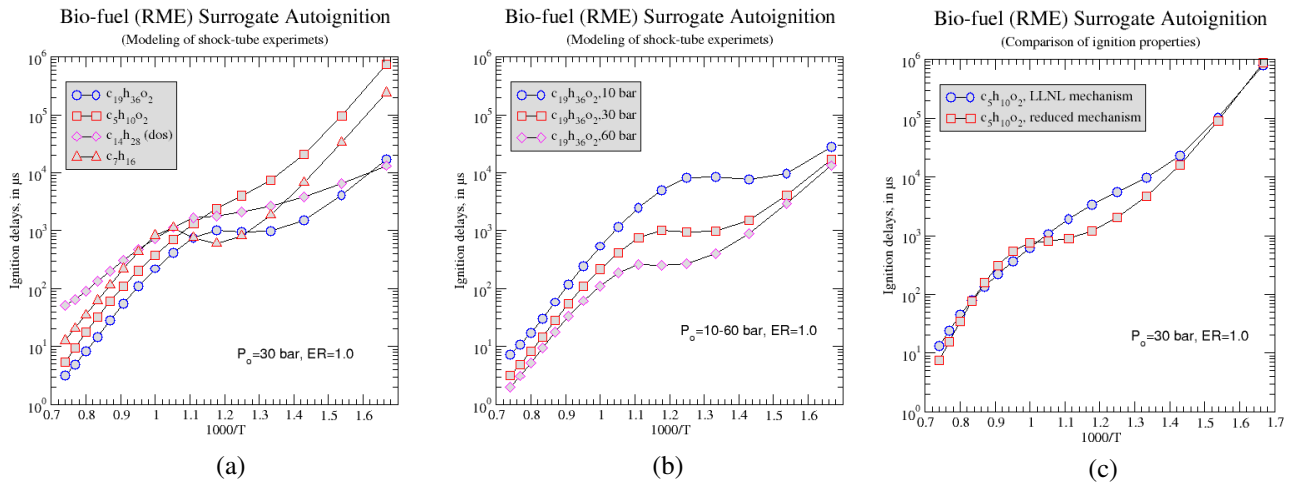The predicted ignition delay times simulating shock-tube experiments are plotted in Fig. 5.

Figure.5: Auto-ignition properties for a) RME, its constituent components, n-heptane, mb, and diesel oil surrogate; b) RME at different pressures; c) RME calculated using detailed and reduced chemical mechanisms.

To define leading stages of the RME combustion mechanism, the sensitivity analysis with the help of the SENKIN code of Chemkin-2 package [23] has been performed. Since the detailed mechanism for RME oxidation is too large for making sensitivity analysis, it was applied only to the reduced mechanism to reproduce the ignition delays calculated using the detailed mechanism as shown in Fig. 5 c). The results

of the sensitivity analysis are illustrated in Figs. 6-7. The aim of the sensitivity analysis is to confirm the significant pathways of RME oxidation used to construct the reduced mechanism in [1].

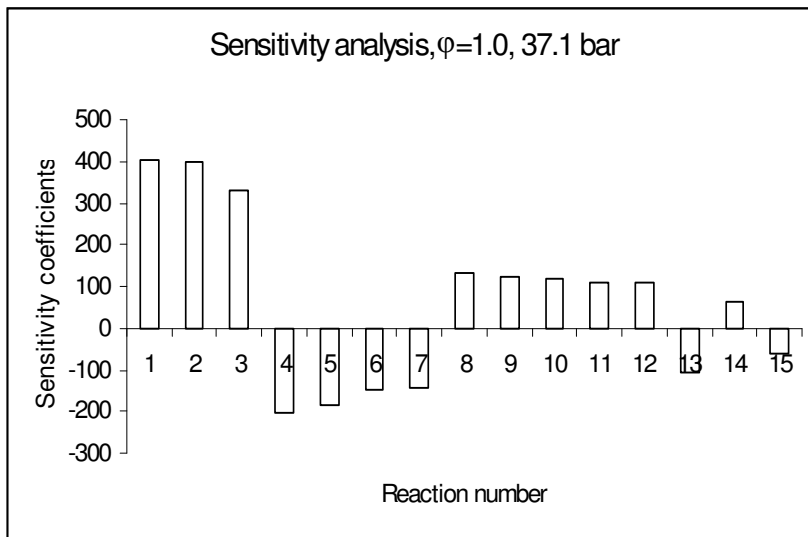|	
1	C5H10O2+HO2=H2O2+mb2j
2	C5H10O2+OH=H2O+mb2j
3	mb2oo=mb2ooh4j
4	C5H10O2+OH=H2O+mb3j
5	HO2+HO2=H2O2+O2
6	CH2O+OH=HCO+H2O
7	C5H10O2+O2=HO2+mb2j
8	CH3+HO2=CH3O+OH
9	mb2ooh4oo=mb4ooh2*o+OH
10	H2O2+M=OH+OH+M
11	CO2+CH3=CH3OCO
12	CH2O+HO2=HCO+H2O2
13	CO+CH3O= CH3OCO
14	C5H10O2+H=H2+mb2j
15	H+O2+N2=HO2+N2

Figure.6: Temperature/reaction rate sensitivity coefficients for the reduced RME oxidation mechanism calculated using SENKIN code: time= 0.002 s, T =970 K, P=37.1 bar, reactions are numbered according to their significance

The results presented in Fig. 6 characterize the ignition process of the stoichiometric RME/air mixture. For this stage, the significant reactions with the largest sensitivity coefficients are mostly the same as those found in [1, see page 6].

1	C5H10O2+HO2=H2O2+mb2j
2	C5H10O2+OH=H2O+mb2j
3	mb2oo=mb2ooh4j
4	HO2+HO2=H2O2+O2
5	C5H10O2+OH=H2O+mb3j
6	CH3+HO2=CH3O+OH
7	H2O2+M=OH+OH+M
8	CH2O+OH=HCO+H2O
9	C5H10O2+O2=HO2+mb2j
10	mb2ooh4oo=mb4ooh2*o+OH
11	CH2O+HO2=HCO+H2O2
12	CO2+CH3=CH3OCO
13	CO+CH3O= CH3OCO
14	CH4+HO2=CH3+H2O2
15	H+O2+N2=HO2+N2
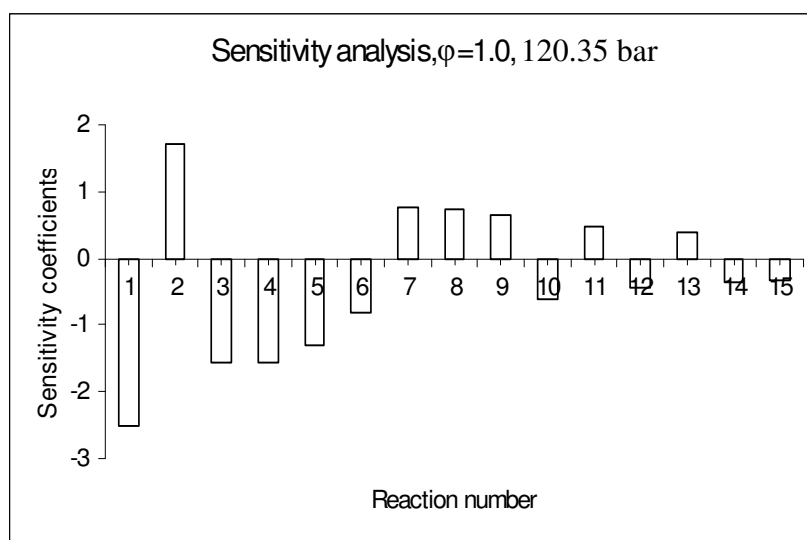
Figure.7: Temperature/reaction rate sensitivity coefficients for the reduced RME oxidation mechanism calculated using SENKIN code: time= 0.0715 s, T =2921 K, P=120.35 bar, reactions are numbered according to their significance

The results presented in Fig. 7 characterize the final (close to equilibrium) stage of combustion of the same mixture illustrating the change of main reaction pathways. As expected, the largest sensitivities occur during the ignition stage of combustion development.

Spray Combustion Modeling

Numerical modeling of combustion in the constant volume offers an easy method for estimating efficiency of fuels ignition quality that can be validated using constant volume combustion vessel experiments, see e.g. [24]. The spray characteristics (a penetration length, etc.), injection timings and ignition delays have a considerable impact on emissions formation in diesel engines. The calculations were carried out for RME and diesel oil for comparison: temperature and soot distributions at different instants in the chamber at "standard" conditions are presented in Figs 8-9, illustrating the details of spray formation, ignition, combustion, and soot formation. Simulation conditions and injection parameters are: P_0= 50 bar, T_0=800 K; m_{inj}= 6 mg, and t_{inj}=1.27 ms, respectively. The 2-D simulations were performed on a mesh consisting of ~20, 000 cells representing the constant volume, which size was selected to prevent the substantial pressure rise when combustion proceeds.

By comparing the spray core penetration, one can conclude that its value for bio-diesel is obviously longer than for typical diesel oil, as showing in Fig. 8. That's because the bio-diesel has worse vaporization characteristics due to a higher critical temperature (764 K), compared to the diesel's (736 K as specified for diesel oil model included into the fuel library of the KIVA-3V code). Fig. 8 also illustrates that bio-diesel combustion results in the lower in-cylinder temperature compared with the diesel oil.
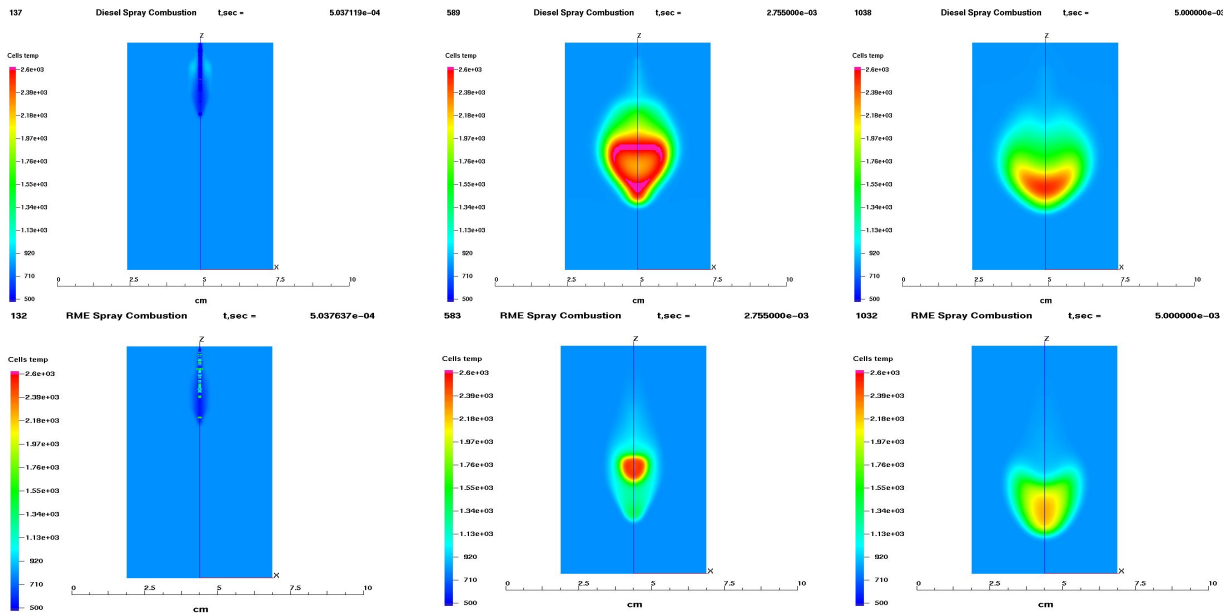
Figure.8 Comparison of gas temperature at different instants for diesel and bio-diesel fuels

Fig. 9 displays the predicted soot distributions at different instants and locations along the fuel spray, showing regions of a high soot mass concentration, SMC, moving along the spray with time. The SMC values in the case of bio-diesel reach the peak value of 5.3 g/m^3 around 2.75 ms, compared to the peak SMC value of diesel of about 136 g /m^3. However, as time increasing, the bio-diesel fuel combustion retains more soot than diesel oil due to the lower in-cylinder temperature that reduces the soot oxidation rate. This effect will be more pronounced at the diesel engine conditions when more fuel will be injected.
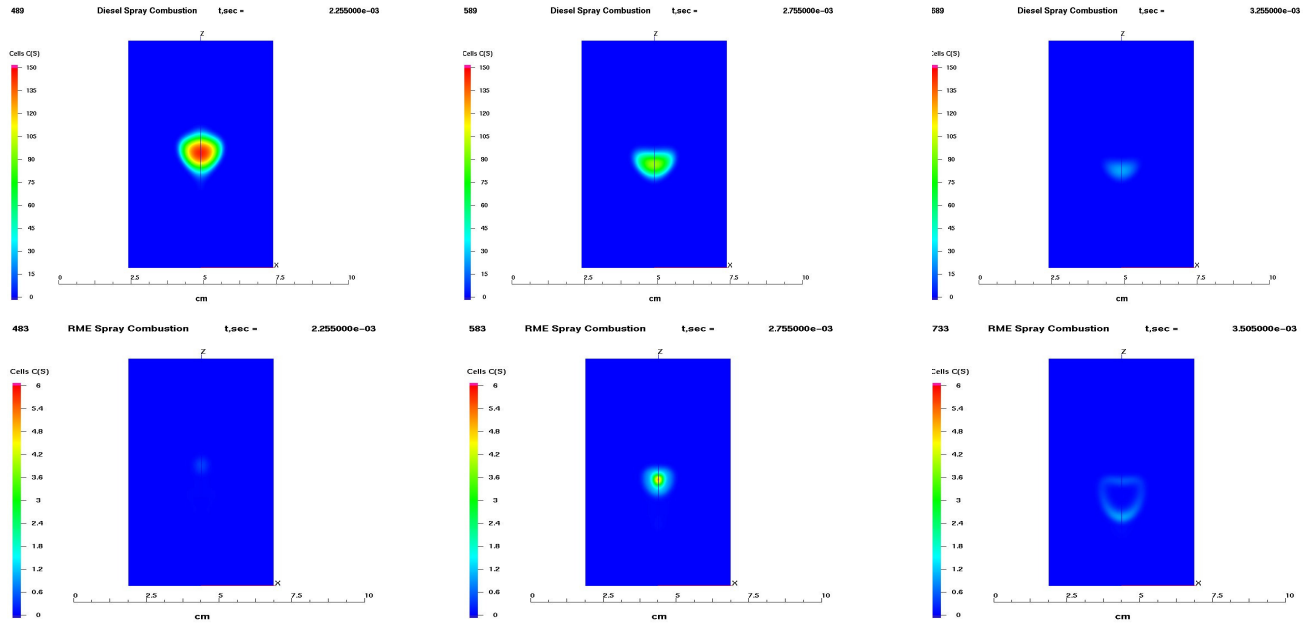
Figure.9: Comparison of soot distributions at different instants for diesel and bio-diesel fuels

Engine Modeling

Finally, the computational model has been applied to the axisymmetric bowl-in-piston engine geometry with a peak in the centre of the bowl. The studied engine was Volvo D12C diesel DI engine. Details of the combustion chamber and injector specifications are given in Tab. 4. The fine 60-degree sector mesh consisted of ~77, 000 cells close to TDC is shown in Fig.10. The mesh was constructed using the pre-processor of the KIVA-3V code.

Bore	$131 \cdot 10^{-3}$ m
Stroke	$150 \cdot 10^{-3}$ m
Squish	$1.85 \cdot 10^{-3}$ m
Connecting rod	$260 \cdot 10^{-3}$ m
Injector nozzle dia($\varnothing$)	$0.235 \cdot 10^{-3}$ m
Engine speed	1000 rmp
Start of injection	-5.5 cad ATDC
Injection duration	9.2 cad
Injection mode	Pilot + main
Injected mass/stroke	60.8 mg
Initial pressure	1.03 bar
Initial temp	330 K
Included angle of spray	145 deg
Spray cone ½ angle	12.5 deg
Initial droplet temp	350 K

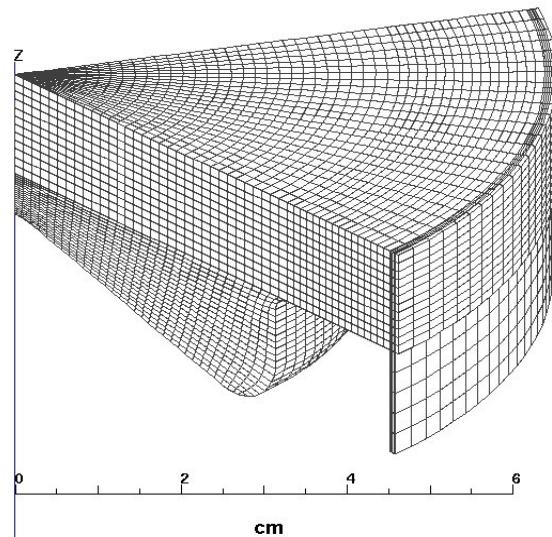Table.4: Volvo D12C diesel engine and fuel injection specifications

Figure.10 The fine 60-degree sector meshes for the Volvo D12C diesel engine. The piston crevice region is included

The modeling results representing the averaged in-cylinder parameters (pressure, rate of heat release, RoHR, and soot mass concentration) are presented in Fig. 11 both for conventional diesel and bio-diesel fuels.
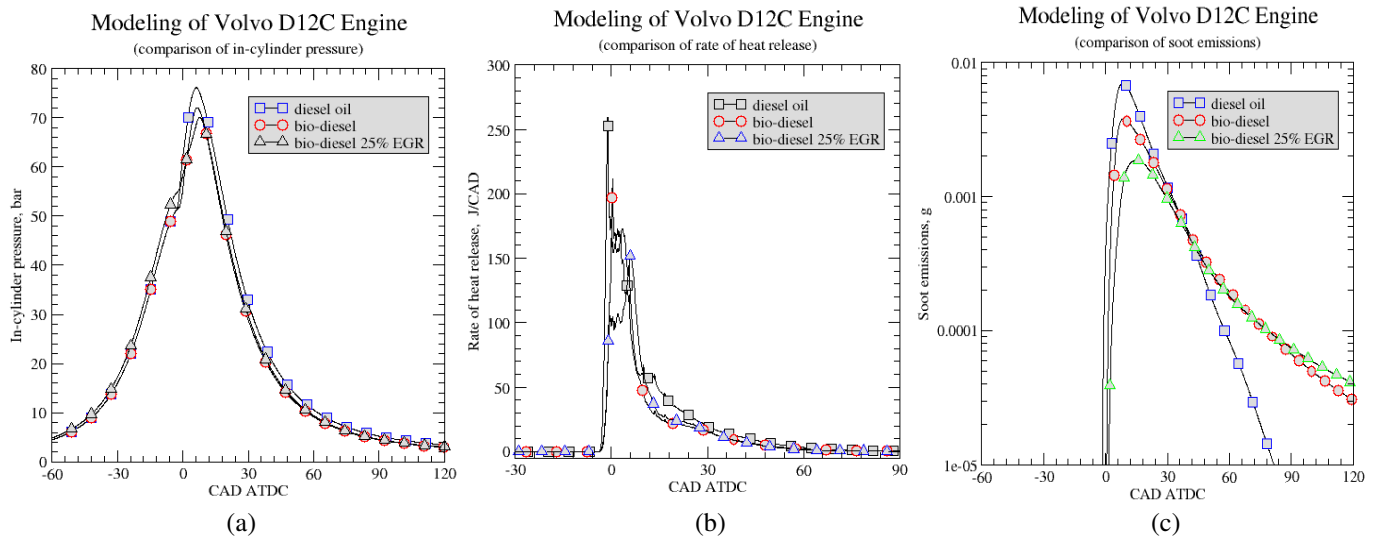

Figure 11: Engine simulation results: averaged in-cylinder parameter vs. CAD histories for a) in-cylinder pressure; b) rate of heat release; c) soot concentration

As shown in Fig. 11, bio-diesel fuel causes: a) a lower in-cylinder pressure, b) a lower rate of heat release during the combustion process compared to the conventional diesel oil. That's due to the fact that bio-diesel has a lower heating value (37.2 MJ/kg) when compared to the diesel oil value of 42.6 MJ/kg. The lower peak soot emission for bio-diesel fuel was predicted together with the higher soot level in the exhaust gas as shown in Fig. 11 c). These effects become more pronounced in the presence of 25% EGR.

In Figs 12-14, the predicted in-cylinder temperatures, soot and NO emissions for conventional diesel oil and bio-diesel (RME) are displayed. Three different CAD instants were selected to exhibit the combustion and emission formation development. Temperature distributions illustrate that combustion starts in the region above the bowl, develops more rapidly for conventional diesel oil and propagates then into the bowl and squish regions. Similar combustion features were predicted in the case of the RME, but maximum temperatures were calculated lower for the RME case, ~2670 K, compared with ~2790 K for the diesel oil. From Fig. 13 follows that the maximum values of soot concentration was predicted lower for the RME case compared with the diesel oil. This is in a compliance with the averaged values presented in Fig. 11c). The NO distributions presented in Fig. 14 illustrate that amount of NO were predicted lower in the RME case due to the lower combustion temperature.

Emission formations were also analyzed using the concept of the φ-T maps [25], which shows soot and NO formation tendencies as functions of φ and T as sown in Fig 15. In-cylinder parameters predicted using KIVA-3V code are presented in these maps by clusters of points representing different regions in the cylinder during the combustion process at different CAD. The backgrounds in the maps were generated from the RME kinetic simulations using the SENKIN code within the specified φ-T ranges. If cell clusters are not intersecting the regions of emission formations, it corresponds to the low emission combustion process in the engine. The transient (dynamic) maps [26] were used in the analysis.

diesel oil

(a)

diesel oil

(b)

diesel oil

(c)

RME

(a)

RME

(b)

RME

(c)
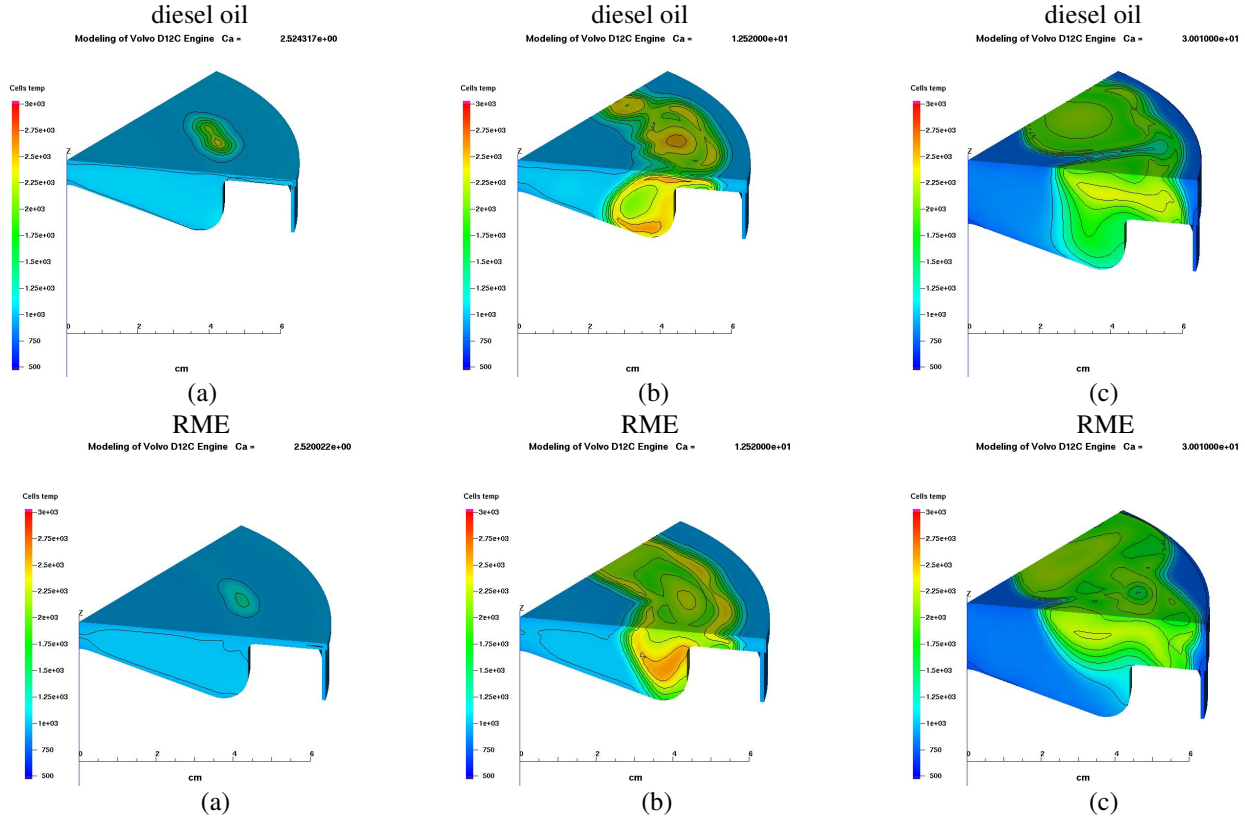
Figure 12: In-cylinder temperature distributions for diesel oil and RME at: a) 2.5; b) 12.5; c) 30 CAD ATDC

diesel oil

(a)

diesel oil

(b)

diesel oil

(c)

RME

(a)

RME

(b)

RME

(c)
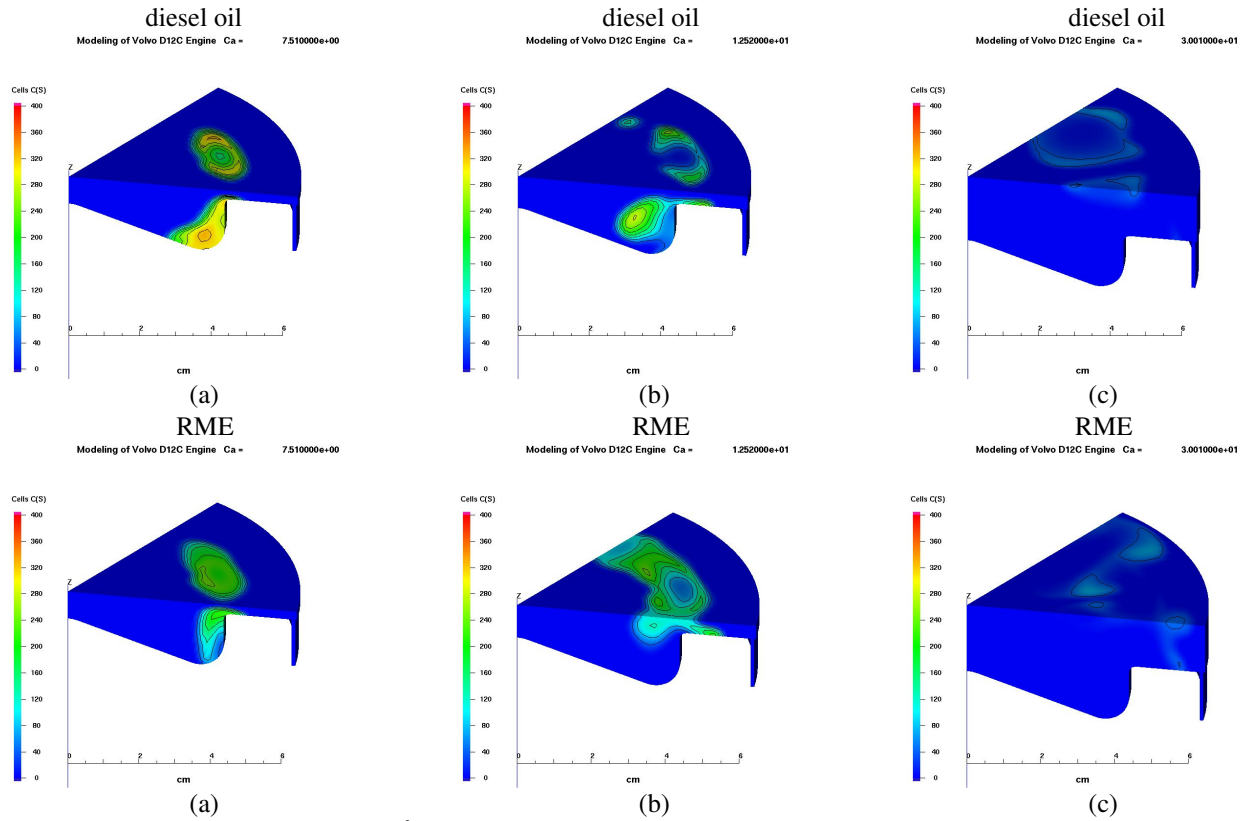
Figure 13: Soot concentration (in g/m^3) distributions for diesel and bio-diesel fuel at: a) 2.5; b) 12.5; c) 30 CAD ATDC
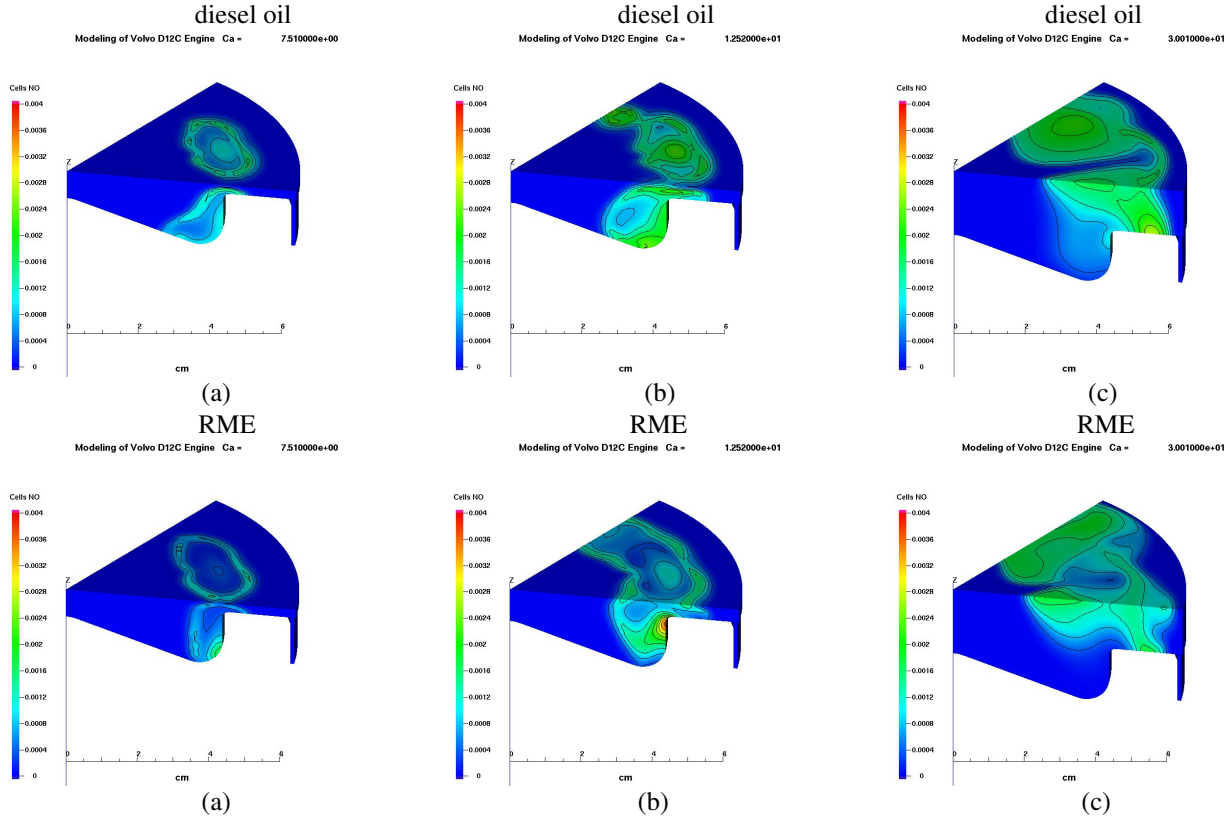
Figure 14: NO mass fraction distributions for diesel and bio-diesel fuel at: a) 2.5; b) 12.5; c) 30 CAD ATDC

(a) -2.5 CAD ATDC   (b) 0 CAD ATDC   (c) 17.5 CAD ATDC

Figure 15 Analysis of emission formation using φ-T parametric maps for pure bio-diesel fuel and bio-diesel with 25% EGR, SOI = -5.5 CAD ATDC, rpm = 2000, in–cylinder conditions correspond to -2.5, 0 and 17.5 CAD ATDC

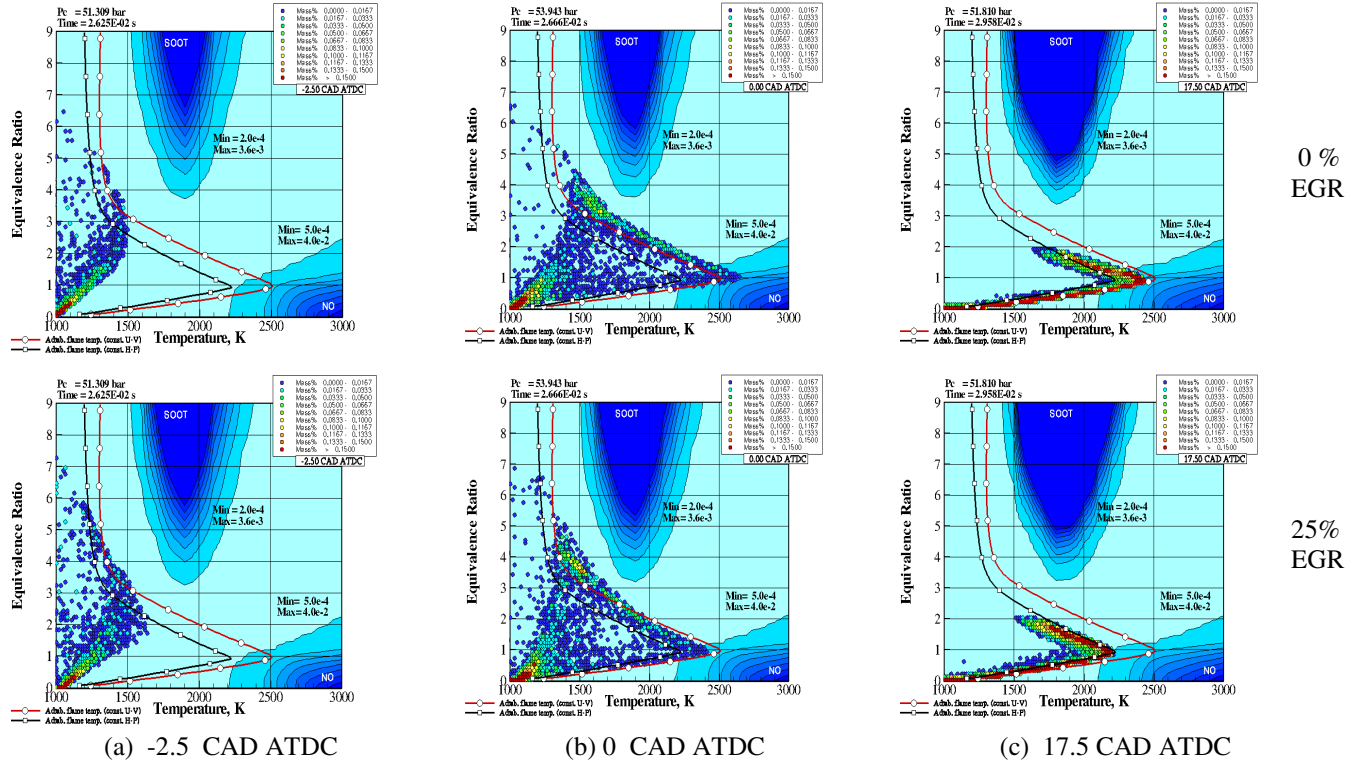The effect of NO reduction in the presence of EGR due to the reduced combustion temperature is well illustrated, if to compare upper and lower rows of Fig 15. The width of the soot and acetylene peninsulas for RME was predicted wider than those in the case of conventional diesel oil as reported in [27]. Due to the presence of the oxygen in the RME molecule, the minimum of φ-value at which soot was formed, calculated to be about 3, while for the diesel oil case it was about 2. Contrary, the width of the C_6H_6 peninsula was predicted narrower that reflects the difference in the soot formation mechanism. To improve the modeling, further refinement of RME surrogate model is required. To make this refinement, the experimental data are necessary.

CONCLUSION

1. The data sets for the liquid bio-diesel (RME) properties (fuel and vapor enthalpies, latent heat of vaporization, vapor pressure, liquid viscosity, surface tension and thermal conductivity) which required for CFD combustion modeling were constructed.

2. The chemical RME combustion mechanisms (detailed and reduced) were developed based on the decomposition of RME, $C_{19}H_{34}O_2$, or $C_{19}H_{36}O_2$ into constituent components, md, C_7H_{16}, $C_5H_{10}O_2$ and C_3H_4. Sub-mechanisms for the constituent components are validated using shock-tube and flame propagation experimental data. The reduced mechanism (88 species, 363 reactions) for 3-D CFD modeling has been constructed and "tuned" using sensitivity analysis.

3. Using the bio-diesel surrogate models, the numerical simulations of combustion development and emission formations in the constant volume and Volvo D12C were performed and the predictions were compared with the same values calculated for conventional diesel oil. The simulation results illustrate that theoretical RME combustion efficiency can be achieved with low soot and NO concentrations if moderate ERG loads are used.

4. Coupled emission map concept and CFD simulations were applied to find out efficient engine operation and low emission formation parameters.

5. To improve the modeling, further refinement of RME surrogate model is required based on the comparison of prediction with experimental data.

REFERENCE

[1]J.L. Brakora, Y. Ra, R.D. Reitz, M. Joanna, C.D. Stuart, *"Development and validation of a Reduced Reaction Mechanism for Biodiesel-Fueled Engine Simulations,"* SAE Paper 2008-01-1378 (2008)
[2]H.J. Curran, S.L. Fischer, F.L Curran, *Int. J. Chem. Kinet. 32(2000) 741-759.*
[3]http://www-cmls.llnl.gov/?url=science_and_technology-chemistry-combustion-mbutanoate.
[4] ftp://ftp.technion.ac.il/pub/supported/aetdd/thermodynamics/
[5]K.H. Lam, A. Violi, *"Thermal Decomposition of Methyl Butanoate: An Initial study of a Biodiesel Fuel Surrogate,"* J.

Org. Chem. 2008, 73, 94-101

[6] T.E. Daubert, R.P. Danner, *"Physical and Thermodynamic Properties of Pure Chemicals",* Part 4 (1989).

[7] D. Rochaya, *"Numerical Simulation of Spray Combustion using Bio-mass Derived Liquid Fuels,"* Cranfield University, PhD Thesis, Bedfordshire (2007).

[8] C.R Reid, M.J Prausnitz, E.B. Poling, *"The Properties of Gases and Liquid,"* 4th ed, McGraw-Hill, Inc. (1987).

[9] http://www.ddbst.de/new/Default.htm, Biodiesel Related Data (2006).

[10] Y. Ra, R.D Reitz, J. McFarlane, C.S Daw, *"Effects of Fuel Physical Properties on Diesel Engine Combustion using Diesel and Bio-diesel Fuels,"* SAE Paper 2008-01-1379 (2008)

[11]J.A. Riddick, W.B. Bunger, *"Organic Solvents: Physical Properties and Methods of Purification"*, 3rd ed., Wiley Interscience, New York (1970).

[12]C. Baroncini, F. DiFilippo, G. Latini, M. Pacetti, *"Organic Liquid Thermal Conductivity: A Prediction Method in the Reduced Temperature Range 0.3 to 0.8,"* *Int. J. of Theomorphic*. 2(1), 21 (1981).

[13]J.O. Peter, *Collective Drop Effects on Vaporizing Liquid Sprays*, PhD Thesis, Princeton University, New Jersey (1981).

[14]J. Gustavsson, V.I. Golovitchev, *"Spray Combustion Simulation Based on detailed Chemistry Approach for Diesel Fuel Surrogate Model,"* SAE Paper 2003-01-1848 (2003)

[15]A.A. Amsden, *"KIVA-3V: A Block-structured KIVA Program for Engines with Vertical or Canted Valves,"* LA-13313-MS, UC-1412, Los Alamos, New Mexico 87545 (1997)

[16]V.I Golovithev, N. Nordin, R. Jarnicki and J.Chomiak. *"3-D Diesel Spray Simulation using a New Detailed chemistry Turbulent Combustion Model,"* SAE Paper 2000-01-1891 (2000).

[17]P. Glarborg, R.J. Kee, J.F. Grcar, J.A. Miller, *"PSR: A Fortran Program for Modeling Well-Stirred Reactors,"* SANDIA Report SAND86-8209 (1992).

[18]R.O. Fox, *"On the Relation Between Lagrangian Micromixing Models and Computational Fluid Dynamics,"* Chemical Engineering and Processing, 37: 521-535 (1998)

[19]C. Aubry, J. Villermaux, J. Chemical Engineering Science, 30, p.457 (1975)

[20]http://www.tfd.chalmers.se/~valeri/MECH.html

[21]J. Fredriksson, M. Bergman, V.I. Golovitchev, I. Denbratt, *"Modeling the Effect of Injection Schedule Change on Free Piston Engine Operation"*, SAE Paper 2006-01-0449 (2006).

[22]Y.L.Wang, C. Ji, A.T. Holley, F.N. Egolfopoulos, T.T. Tsotsis, H.J. Curran, *"Studies of Combustion Characteristics of Biofuels in Premixed and Non-premixed Flames"*, 2007 Fall Meeting of WSS/CI-Paper #07F-49 (2007).

[23]A.E. Lutz, R.J. Kee, J.A. Miller, *"SENKIN: A FORTRAN Program for Predicting Homogeneous Gas Phase Chemical Kinetics with Sensitivity Analysis,"* 1988:SAND 89-8009, UC-4 (1988).

[24]J. Senda, T. Ikeda, T. Haibara, S. Sakurai,Y. Wada, H. Fujimoto, *"Spray and Combustion Characteristics of Reformulate Biodiesel with Mixing of Lower Boiling Point Fuel,"* SAE Paper 2007-01-0621 (2007).

[25]K. Akihama, Y. Takatori, K. Inagaki, S. Sasaki, A M.Dean, *"Mechanism of the Smokeless Rich Diesel Combustion by Reducing Temperature"*, SAE Paper 2001-01-0655 (2001).

[26]M. Bergman, V.I. Golovitchev, *"Application of Transient Temperature vs. Equivalence Ratio Emission Maps to Engine Simulations"*, SAE Paper 2007-01-1086 (2007).

[27]J. Kusaka, L. Montorsi, V.I. Golovitchev, I. Denbratt, *"Numerical Simulation on Combustion in a Heavy Duty Diesel Engine"*, FISITA 2006 World Automotive Congress, Paper F2006P398 (2006)

APPENDIX

The detailed methyl butanoate's mechanism involving 264 species and 1219 reactions has been created and validated at LLNL [2]. The RME mechanism reduced for CFD application is listed below. The following explains the species names in the methyl butanoate and RME mechanisms in LLNL notations:

-Carbon are numbered starting with 1= carbonyl carbon.

-m denotes the carbon in the methoxy group

- Groups attached to a given carbon atom are listed after the number or letter labeling that carbon atom.

- j denotes a radical site. For example, mb3j4ooh is methyl butanoate with a hydroxyl group attached to the terminal carbon (number 4) and a hydrogen atom missing from the carbon next to the terminal one (number 3)

-*o denotes an oxygen atom attached via a double bond

- d denotes a double bond connecting carbon n and carbon n+1. e.g, mb2d has a double bond between carbon 2 and carbon 3.

Example:

rme: ch3-(hc=ch)$_2$-(ch2)$_{12}$-(c=o)-o-ch3

md: ch3-(hc=ch)-(ch2)$_7$-(c=o)-o-ch3

mb: ch3-o-(c=o)-ch2-ch2-ch3

mp: ch3-o-(c=o)-ch2-ch3

me:ch3-o-(c=o)-ch3

mb4oo2*o:ch3-o-(c=o)-(c=o)-ch2-ch2-(o-oh)

mb2j:ch3-o-(c=o)-c*h-ch2-ch3, etc.

The fragment of the reduced RME mechanism:

REACTIONS, j	Aj	nj	Ej
rme+ O2 => md+ c5h10o2+C3H4	5.00E+11	0.0	10500.0
mb2j + H = c5h10o2	1.00E+14	0.0	0.0
mb3j + H = c5h10o2	1.00E+14	0.0	0.0
c5h10o2 + O2 = HO2 + mb3j	2.00E+13	0.0	51050.0
c5h10o2 + OH = H2O + mb3j	4.68E+07	1.61	-35.0
c5h10o2+C2H5=C2H6+mb3j	5.00E+11	0.0	10400.0
c5h10o2+C2H3=C2H4+mb3j	4.00E+11	0.0	16800.0
me2j + C2H5 = c5h10o2	8.00E+12	0.0	0.0
c5h10o2 + O2 = HO2 + mb2j	4.00E+13	0.0	41300.0
c5h10o2 + CH3 = CH4 + mb2j	2.01E+11	0.0	7900.0
c5h10o2 + H = H2 + mb2j	6.52E+14	0.0	7300.0
c5h10o2 + HO2 = H2O2+ mb2j	4.32E+12	0.0	14400.0
c5h10o2 + O = OH+ mb2j	2.20E+13	0.0	3280.0
c5h10o2 + OH = H2O + mb2j	1.15E+11	0.5	63.0
c5h10o2 + C2H3 = C2H4 + mb2j	4.00E+11	0.0	14300.0
c5h10o2 + C2H5 = C2H6+ mb2j	2.00E+11	0.0	7900.0
c5h10o2 + mb2oo = mb2ooh + mb2j	2.16E+12	0.0	14400.0
mp2d+ CH3 = mb2j	1.00E+10	0.0	7600.0
mb2d + H = mb2j	1.00E+13	0.0	2900.0
mb2j+ O2 = mb2oo	1.41E+13	0.0	0.0
HO2+ mb2j= OH+ mb2o	7.00E+12	0.0	-1000.0
mb2oo+ HO2 = mb2ooh + O2	1.75E+10	0.0	-3275.0
mb2oo+ mb2oo= O2+ mb2o+ mb2o	1.40E+16	-1.6	1860.0
mb2oo+ mb2j= mb2o+ mb2o	7.00E+12	0.0	-1000.0
mb2oo+ CH3 = CH3O+ mb2o	7.00E+12	0.0	-1000.0
mb2ooh= mb2o + OH	6.00E+15	0.0	42540.0
ch3oco + C3H7= c5h10o2	1.81E+13	0.0	0.0
mp2d+ CH3 = c2h3co+ CH2O+ CH4	4.52E-01	3.65	7154.0
C2H3 + ch3oco= mp2d	1.00E+13	0.0	0.0
mp2d+ H= c2h3co +CH2O+ H2	9.40E+04	2.75	6280.0
mp2d + O = ch3oco + CH2CHO	5.01E+07	1.76	76.0

REACTIONS, j	Aj	nj	Ej
md=> mp2d+C7H16	5.00E+11	-0.61	10500.0
C2H3 + O2 = CH2CHO + O	3.50E+14	-0.61	5260.0
CO + CH3O = ch3oco	1.50E+11	0.0	3000.0
CO2 + CH3 = ch3oco	1.50E+11	0.0	36730.0
c2h3co = C2H3 + CO	2.04E+14	-0.4	31450.0
mb2oo + H2O2 =mb2ooh + HO2	2.40E+12	0.0	10000.0
mb2ooh+ HO2 =mb2oo+ H2O2	2.40E+12	0.0	10000.0
CH2CO + CH3O = me2j	5.00E+11	0.0	-1000.0
mp2d + O= me2j + HCO	1.58E+07	1.76	-1216.0
me2*o + H = me2j*o + H2	4.00E+13	0.0	4200.0
me2*o + CH3 = me2j*o + CH4	1.70E+12	0.0	8440.0
me2*o + HO2 = me2j*o + H2O2	2.80E+12	0.0	13600.0
me2*o + OH = me2j*o + H2O	2.69E+10	0.76	-340.0
me2*o + O = me2j*o + OH	5.00E+12	0.0	1790.0
me2*o + C2H5 = mb2o	1.50E+11	0.0	11900.0
ch3oco+ CO= me2j*o	1.50E+11	0.0	3000.0
C3H6 + ch3oco = mb3j	1.06E+11	0.0	7350.0
mb2d + H = mb3j	1.00E+13	0.0	2900.0
CH3 + mp2d3j= mb2d	1.00E+13	0.0	0.0
C2H2 + ch3oco = mp2d3j	1.61E+40	-8.58	20330.0
mb2oo = mb2ooh4j	6.00E+10	0.0	22000.0
mb2ooh4j + O2 = mb2ooh4oo	4.52E+12	0.0	0.0
mb2ooh4oo = mb4ooh2*o + OH	9.98E+10	0.0	20350.0
mb4ooh2*o =CH2O + mp3j2*o + OH	1.50E+16	0.0	42000.0
CH2CO + ch3oco = mp3j2*o	1.00E+11	0.0	9200.0
mb2d + CH3 = c5h7o2 + CH4	1.00E+12	0.0	7300.0
mb2d + H= c5h7o2 + H2	3.70E+13	0.0	3900.0
c5h7o2+ OH = mb2d + O	7.00E+11	0.0	29900.0
mb2d + OH= c5h7o2+ H2O	3.00E+13	0.0	1230.0
mb2d + HO2 = c5h7o2+ H2O2	1.50E+11	0.0	14190.0

Reaction rates in cm^3 mol cal unit, k=AT^{n}exp(-E/RT)